9-1-2000

The effect of Stochastic cloud structure on the icing process

A. R. Jameson
RJH Scientific, Inc.

Alexander Kostinski
Michigan Technological University

Recommended Citation

Jameson, A. R., & Kostinski, A. (2000). The effect of Stochastic cloud structure on the icing process. *Journal of the Atmospheric Sciences, 57*(17), 2883-2891. http://dx.doi.org/10.1175/1520-0469(2000)057<2883:TEOSCS>2.0.CO;2
Retrieved from: https://digitalcommons.mtu.edu/physics-fp/244

Follow this and additional works at: https://digitalcommons.mtu.edu/physics-fp

 Part of the Physics Commons

The Effect of Stochastic Cloud Structure on the Icing Process

A. R. JAMESON

RJH Scientific, Inc., Alexandria, Virginia

A. B. KOSTINSKI

Department of Physics, Michigan Technological University, Houghton, Michigan

(Manuscript received 21 January 1999, in final form 9 July 1999)

ABSTRACT

Current understanding of the icing process through collisions between a surface and supercooled cloud droplets is based upon two factors. First, for a given temperature, when the cloud liquid water content, W, exceeds a critical value, w_c (the Schumann–Ludlam limit), the ice that collects, whether on the surface of a hailstone or on the wing of an aircraft, changes from lower densities to values close to that of water. Second, it is assumed that cloud droplets are dispersed in space as uniformly as randomness allows (''Poissonian'' clouds).

It is now becoming well established, however, that clouds are not Poissonian. Rather, the droplets are ''clustered'' so that clouds consist of interspersed regions both rich and deficient in droplets. This is significant because it leads to a much broader probability distribution (pdf) of droplet counts than would be the case for a Poissonian cloud. That is, the ratio of the variance to the mean is much greater than unity (the Poissonian value). As a consequence, droplet clustering also produces a bunching or clustering of W as well as leading to ''patchy'' clouds. This paper explores the effect of this patchiness on the icing process.

Results show that clustering is important for at least three reasons. First, it produces a broadening of the pdf of W. Second, this broadening means that $W > w_c$ by significant amounts over significant distances even when a Poissonian cloud would exclude such a possibility for the same average water content. Third, these spatial inhomogeneities introduce a ''memory'' into the icing process that is lacking in Poissonian clouds.

1. Introduction

It is well known that the density of accreted ice that forms as supercooled water droplets impact a surface depends upon the velocity of the object, the ambient air temperature, and the liquid water content, W, of the cloud, among other factors (e.g., Macklin 1962). For a set of fixed conditions, this has led to the identification of a ''critical'' water content (the Schumann–Ludlam limit), w_c, when the nature of the collected ice changes from a situation when water freezes as rapidly as it is collected ($W < w_c$; the so-called dry-growth regime), to the case when excess water is supposed to be shed when $W > w_c$ (the so-called wet-growth regime; Schumann 1938; Ludlam 1958).

While conceptually correct, subsequent laboratory experiments show that reality is more complex. That is, excess water that cannot be frozen rapidly enough is not simply discarded but is often captured in a crystal matrix of ''spongy'' ice (List 1959, 1960; Macklin 1961). When such ice subsequently freezes it forms a high-density coating. Macklin (1962) shows that the greater the impact speed and droplet size, the greater the density of accreted ice. This is countered by colder surface temperatures that promote the formation of lower-density ice. The net effect is that above the Schumann–Ludlam limit, dense ice is inevitable, while below that limit, lower-density rime ice becomes more likely.

Such a transition is relevant not only for understanding the fundamentals of hailstone growth but also for distinguishing conditions likely to produce relatively low-density, benign dry rime ice as opposed to those likely to generate the much more dangerous high-density ice capable of altering the lift of aircraft wings.

While it may sometimes be possible to identify dry growth conditions simply by knowing the mean cloud water content and temperature if the clouds are ''Poissonian''—that is, if the droplets are distributed spatially as uniformly as randomness allows—ambiguities are likely in most real clouds because of droplet clustering, that is, because natural clouds are not ''uniform'' but ''patchy'' (e.g., Jameson et al. 1998; Kostinski and Jameson 2000).

In this work, we quantify the meaning of patchiness for cloud droplets of one size and then extend this con-

Corresponding author address: Dr. A. R. Jameson, RJH Scientific, Inc., 5625 N. 32nd St., Arlington, VA 22207-1560.
E-mail: jameson@rjhsci.com

cept to explore the patchiness of clouds themselves, that is, of the water content. It is shown that such patchiness leads to a significant increase in frequency of $W > w_c$ than would be expected for Poissonian clouds in which the water content fluctuates very narrowly about the mean value. That is, simply knowing the mean W is not sufficient. One must also know the ratio of the variance to the mean water content for a more complete description of the icing process. The patchiness of clouds not only likely explains much of the fine structure observed in cross sections of hailstones but, on a more practical note, likely contributes to unsafe aircraft icing conditions even when, for the same mean water content, a Poissonian cloud would preclude any danger.

2. Patchy clouds and the icing process

If we represent the random number of droplets of a single size in a unit volume by n, say, then for a statistically homogeneous random field, the joint probability $P(1, 2)$ of finding two particles in small volumes dV_1 and dV_2 is given by (e.g., see Green 1969, 62–63)

$$P(1, 2) = \overline{n}^2\, dV_1\, dV_2\, [1 + \eta(l)], \qquad (1)$$

where $\eta(l)$ is the so-called pair correlation function (in the theory of liquids) or the two-point correlation function (in astronomy). (Note, however, that statistical homogeneity does *not* imply nor require physical homogeneity. Patchy, physically inhomogeneous clouds can be fully consistent with statistical homogeneity.) Moreover, it is often assumed in many fields of science that over some interval, usually much greater than some characteristic correlation length, a physical process is often well described by statistical homogeneity (i.e., the mean and the variance are unaffected by shifts in the choice of origin); that is, no ''trend'' appears whether it be light-years in the case of astronomy or the dimensions of molecules in liquids.

For clouds, $\eta(l)$ can be estimated from a series of measurements of the number of droplets in a unit volume of space by

$$\eta(l) \equiv \frac{[\overline{n(l)n(0)} - \overline{n}^2]}{\overline{n}^2} = \frac{\overline{n(l)n(0)}}{\overline{n}^2} - 1. \qquad (2)$$

For droplets that are distributed in space such that $n(l)$ are all independent for all l (as would be the case for the Poisson distribution), then, obviously, $\eta \to 0$. However, when $\eta \neq 0$, we may then say that the droplets are ''correlated'' [(1)] and ''clustered'' [(2)] in that $\langle n(l)n(0)\rangle$ is either greater or less than $(\overline{n})^2$.

This discussion is not new and is presented in a series of articles with regard to rain (Kostinski and Jameson 1997; Jameson and Kostinski 1998; Kostinski and Jameson 1999; Jameson et al. 1999; Jameson and Kostinski 1999b, 2000) and with regard to clouds (Jameson et al. 1998; Kostinski and Jameson 2000). Simply put, clustering of cloud droplets has been observed in a number of clouds (Paluch and Baumgardner 1989; Baker 1992; Jameson et al. 1998; Kostinski and Jameson 2000) in no small part because of the ubiquity of convective turbulence in clouds. While turbulence is often thought to promote smoothing through mixing, recent numerical studies by Wang and Maxey (1993) and Shaw et al. (1998) clearly demonstrate that for particles with a small but significant inertia, such as cloud droplets, the opposite is true, namely, that droplets tend to concentrate in regions of high strain.

What is new in the present work is that we apply a simulation procedure (see appendix) developed for our work on rain to generate Monte Carlo realizations of patchy clouds in order to explore the probability distribution functions of cloud water content with an eye toward its interpretation with respect to the icing process. As a result we show (i) that it is not just the mean W but the ratio of the variance to the mean W that is important, (ii) that this ratio depends upon the length scale associated with the measurement volume, and (iii) that the rate of ice deposition depends on these first two factors through the Schumann–Ludlam limit.

As discussed in Jameson and Kostinski (1999b), $\eta(l)$ defined by (2) serves to highlight two important quantities required for describing and simulating clustering. These are the clustering intensity parameter, $\aleph$, and the autocovariance or ''coherence'' length, χ_l.

First we define $\aleph$ to be

$$\aleph \equiv \frac{\sigma^2}{\mu^2}\left(1 - \frac{\mu}{\sigma^2}\right) = \eta(0)\left(1 - \frac{\mu}{\sigma^2}\right), \qquad (3)$$

where μ and σ^2 are the mean and variance of the number of droplets (per unit volume) over the entire observation domain. Thus, for Poisson distributions, when there is no clustering, $\aleph \to 0$, because $\sigma^2 = \mu$. On the other hand, when clustering is occurring, as described by the geometric distribution, for example, then $\aleph \to \eta(0)[\mu/(1 + \mu)] \to 1$ as can be readily seen by substituting $\eta(0) = \sigma^2/\mu^2$ and by noting that for the geometric distribution $\sigma^2 = \mu + \mu^2$. In fact for other negative binomial distributions, it is easy to show that $\aleph \to \eta(0)[\mu/(m + \mu)] \to 1/m$ as $l \to 0$, where m is the so-called shape parameter of the gamma distribution transformed into a negative binomial distribution by the Poisson mixture process [see Kostinski and Jameson (1997, pp. 2177–2178) for elaboration and discussion]. Consequently, the larger the $\aleph$, the smaller the m. Because of the nature of the gamma distribution, this in turn means that as $\aleph$ increases, m decreases and the resulting shape of the distribution of droplets per unit volume changes such that the tail of the distribution extends to larger concentrations while, simultaneously, the probability densities at small values near zero also increases so that the mean concentration remains unchanged. This, of course, is what is meant by the increased clustering or ''clumping'' of cloud droplets. That is, there are simultaneously both more regions deficient in droplets, interspersed with regions rich in droplets, that is, clus-

ters. Hence, as $\aleph$ increases, the clustering of the cloud droplets increases.

The second variable is the coherence length, χ_l. Defining the autocovariance function for droplets of diameter, D, to be

$$\mathcal{C}_D(l) = \frac{[\overline{n(l)n(0)} - \mu^2]}{\sigma^2}, \tag{4}$$

χ_l is then that length at which $\mathcal{C}_D$ equals $1/e$, where e is the base of natural logarithm. Therefore, χ_l provides a measure of the average ''scale'' or ''size'' of the droplet clustering in clouds. These two variables (χ_l and $\aleph$) are important because they provide a way of characterizing the geometry and intensity of clustering, respectively.

[Here it is worth mentioning that $\eta(l)$ and $\mathcal{C}_D(l)$ are related using (2)–(4) by

$$\eta(l) = \mathcal{C}_D(l)\left(\aleph + \frac{1}{\mu}\right). \tag{5}$$

Thus, for constant μ and χ_l, the correlation lengths where $\eta(l)$ decreases to $1/e$ will depend upon $\aleph$ such that coherence lengths for larger $\aleph$ are longer as will be seen below.]

While it may at first seem that these parameters appear from ''out-of-the-blue,'' there is, in fact, a very good physical explanation for their importance as seen using the correlation–fluctuation theorem, more completely discussed in Kostinski and Jameson (2000), which relates the variance of counts in a given volume to the pair correlation function, integrated over the same volume. While originally developed in statistical physics for the study of density fluctuations in gases and liquids, the derivation is completely general as can be found in Landau and Lifshitz [1980, p. 352, Eq. (116.5)] or Green (1969, pp. 62–63). Specifically, it states that

$$\frac{\overline{(\delta n)^2}}{\overline{n}^2} - \frac{1}{\overline{n}} = \frac{1}{V}\int_V \eta(l)\, dV = \overline{\eta}, \tag{6}$$

where η is the pair correlation function between particle counts in unit volumes V_1 and V_2, separated by distance l as defined by (2), n is the total number of particles in volume V, $\overline{(\delta n)^2}$ is the variance of n, $\overline{n}$ is the mean number of particles in V, and $\overline{\eta}$ is the average over V. Note that our η differs from υ in Landau and Lifshitz (1980) by the factor $\overline{n}/V$. Also note that in the limiting case of no correlation, we recover the Poisson relation $\overline{(\delta n)^2} = \overline{n}$. Thus, according to (6), the mean squared fluctuation of the number of particles in a volume is related to the pair correlation function integrated over the same volume. Then the physical meaning of equation (6) is that given a fixed mean, $\overline{n}$, the variance of number of particles is enhanced by the presence of correlations throughout the sampling volume V. Furthermore, the left-hand side of (6) equals $\aleph$. In addition, dividing by $\overline{n}$ and noting that $\mathcal{C}_D = (\overline{n})^2/\overline{(\delta n)^2} \times \eta$, it follows that

$$1 - \frac{\overline{n}}{\overline{(\delta n)^2}} = \overline{\mathcal{C}_D}, \tag{7}$$

where the bar denotes the average value over V. Since $\overline{\mathcal{C}}_D$ [through (6)] depends inversely upon the size of V, the ratio of the mean to the variance [the lhs of (7)] then also depends inversely upon the size of V [for further discussion see Kostinski and Jameson (2000)]. As V becomes very large, $\overline{\mathcal{C}}_D \to 0$ and, consequently, $\overline{(\delta n)^2} \to \overline{n}$. That is, $\aleph \to 0$. Although clustering is still present at smaller scales, it simply can no longer be observed using sampling volumes that are too large. In this work we choose χ_l as that characteristic dimension of V such that most droplet clustering ($\aleph > 0$) will be observed on scales of order χ_l and smaller.

While there are several techniques in the literature for generating correlated samples, the one used in this study is based upon that given by Johnson (1994), as discussed in detail in the appendix. In these simulations, statistical homogeneity (stationarity) is assumed [For some justification, see appendix A in Kostinski and Jameson (2000)]. As discussed at the end of the appendix, the droplet counts are assumed to obey a variety of distributions depending upon the value of N. Nevertheless, because the simulation of clustering requires correlated samples, apparent ''structures'' can appear at times solely as a result of these correlations. That is, many samples of nearly equal amplitude will be brought into proximity because of correlation. However, since the mean value etc. remain constant throughout the simulations, such structures should not be construed as violations of the assumption of statistical homogeneity. Nor should structures larger than χ_l be construed in themselves to be droplet clusters since clustering will be occurring largely on scales $<\chi_l$ as just discussed.

As Fig. 1 illustrates, this procedure allows us to control the degree of clustering, $\aleph$, while maintaining a constant concentration and a constant autocovariance χ_l. This is important because the coherency of the data series can be maintained even as the frequency distribution of the droplet counts per unit volume is altered, as illustrated in Fig. 2. As discussed above, we note that as $\aleph$ increases, the tails of the distribution extend to increasingly larger values. Since the mean is maintained as well, this requires that the frequencies of lower counts per unit volume must also increase. Hence, there is increasing clustering with increasing $\aleph$ as discussed previously. Note the significant broadening of the droplet frequency distributions compared to a Poisson distribution even when $\aleph$ is quite modest. (Also note that the same value of $\aleph$ is used for all droplet size categories under the assumption that the clustering mechanisms act equally on all droplets of such small sizes leading to interdroplet cross correlation as discussed in the appendix.)

Furthermore, for a constant size of droplets, Fig. 3 illustrates that the procedure yields a good rendition of the autocovariance function actually observed in a real

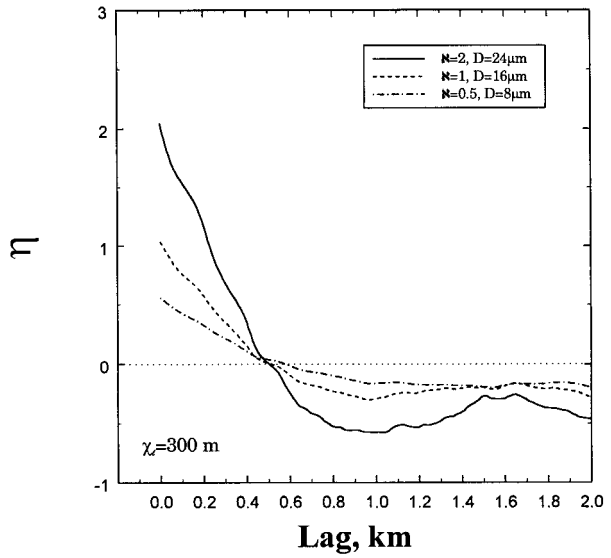

FIG. 1. The pair autocorrelation function η for simulated droplet counts per unit volume for a fixed autocovariance coherence length, χ_l, of 300 m but different degrees of clustering, $\aleph$. The dashed line at zero corresponds to a Poisson distribution.

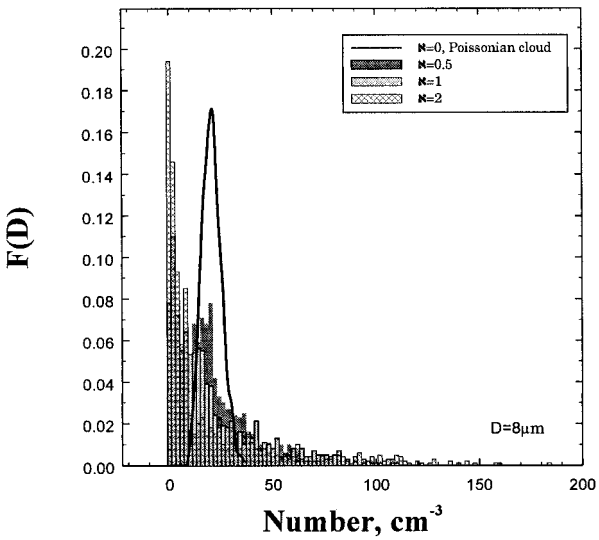

FIG. 2. The frequency distribution of droplet counts for different degrees of clustering, $\aleph$. Note the significant broadening of the distribution even for modest clustering compared to a Poisson distribution as well as the enhanced tail and increased frequencies at low counts as $\aleph$ increases.

cloud (Fig. 7a in Jameson et al. 1998). It is reasonable, therefore, to proceed with the simulation of several different sizes of droplets and, then, to consider the statistical characteristics of the resulting cloud water content.

This is accomplished using four different droplet size categories 8 μm wide centered on mean diameters of 8, 16, 24, and 32 μm. The number of particles per cubic centimeter is calculated assuming a gamma distribution (Pruppacher and Klett 1997, p. 26) and a total cloud water content of 0.5 g m^{-3}. In each simulation the same χ_l and $\aleph$ are applied to each droplet size using the procedure described in the appendix. The χ_l is selected for an exponential autocovariance function to correspond to 30, 90, and 300 m, the latter value corresponding to the ''observed'' curve in Fig. 3.

Unfortunately, at present there are very few measurements of $\aleph$ in clouds. Consequently, we use 0.5 (negative binomial distribution), consistent with the cloud observations in Jameson et al. (1998), but we also extend $\aleph$ to include values as large as 2, as frequently observed in rain (Jameson et al. 1998), just to make certain to include conditions likely to be found in most clouds. A sequence of 1000 realizations of droplet counts per cubic centimeter is then generated for each size category. Furthermore, in order to make the example more concrete, we arbitrarily assign a resolution of 10 m to each realization so that the total path length is 10 km. This does not mean, however, that droplet clustering is occurring over 10-km scales since $\chi_l \ll 10$ km. Finally, we calculate the cloud water content by summing over the drop categories over each interval. This gives 1000 values that can then be used to explore the statistics of W for various χ_l and $\aleph$.

As an example, Fig. 4 is a plot of Monte Carlo simulated clouds for χ_l fixed at 300 m for three different $\aleph$ including $\aleph = 0$ corresponding to a Poissonian cloud. First we note that any structures in Fig. 4 are simply a consequence of correlated fluctuations associated with a constant mean value and should not be construed to be statistical inhomogeneities in which the mean and other properties are changing. Moreover, as $\aleph$ increases, the effect on the cloud water appears to be a ''squeezing'' or confinement of the cloud into narrower regions of increasingly larger W. Even modest clustering

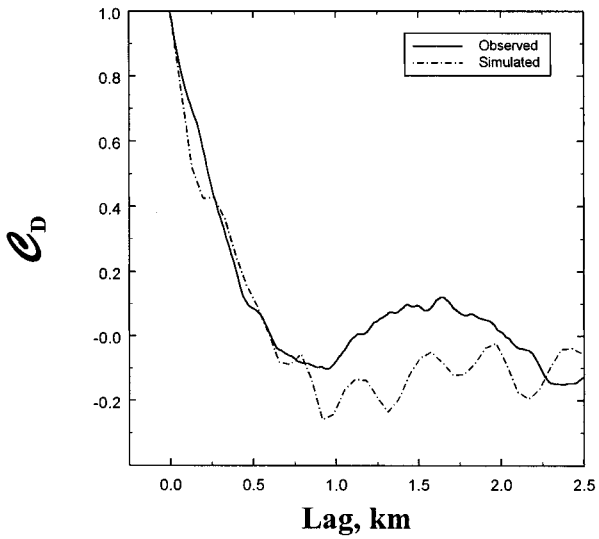

FIG. 3. The autocovariance function for droplet counts, C_D, as observed in a cloud and as reproduced in our simulation.

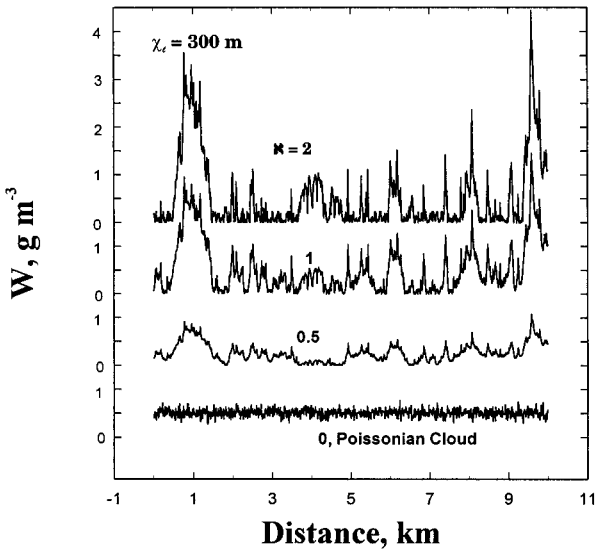

FIG. 4. Spatial series of cloud water content, *W*, for a simulated, statistically homogeneous cloud of correlated droplet counts having a fixed χ_l for different ℵ in clustered clouds as well as for a uniform, Poissonian cloud. Correlated fluctuations in droplet counts produce the structure in *W*, while increasing ℵ of the droplet counts produces increasing magnitudes of the fluctuations in *W* as reflected in Fig. 2.

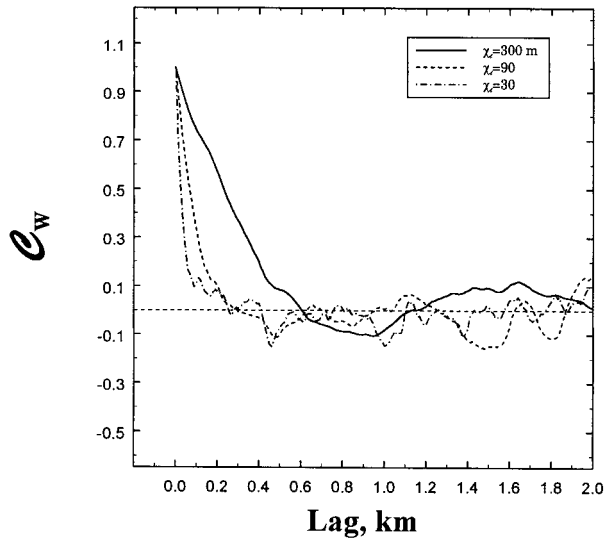

FIG. 5. The autocovariance function for the cloud water content simulated as described in the text for three different χ_l for droplet counts. Note that the same coherence lengths appear as well for *W*.

(ℵ = 0.5) produces a spatial distribution of *W* considerably different from that for a Poissonian cloud having the same mean water content. Obviously such changes due to clustering must be reflected in the probability distribution of *W* as discussed in the next section. There we show results from a simulation of a Poissonian cloud having a subcritical mean water content with regard to dense ice formation and compare it to clouds that are patchy. The implications are then considered.

3. Results

First, the autocovariance functions for the cloud water content, $\mathcal{C}_W$, are computed for the three different χ_l as illustrated in Fig. 5. It turns out that each of these can be well approximated by an exponential distribution (not shown) having the indicated χ_l. The exponential forms for $\mathcal{C}_D$, therefore, appear to carry over to $\mathcal{C}_W$, even though *W* is a sum over the drop categories.

Of greater interest here, however, are the frequency distributions of *W*. In Fig. 6a the distributions are plotted for χ_l = 300 m. The effect of different degrees of clustering (ℵ) of drop counts per unit volume is readily apparent. First, consider the distribution of *W* associated with a Poissonian cloud (Poisson drop concentrations, ℵ = 0) having the same mean of 0.5 g m^{-3} as for the clustered clouds. This distribution is narrowly confined around the mean value. Note that while the droplet counts per unit volume are Poisson, the distribution of *W* in Fig. 6a is actually much narrower having a variance (σ^2) of only 0.0059 g^2 m^{-6}. By contrast, even for ℵ = 0.5, there is a significant broadening of the distributions of *W* (σ^2 = 0.14 g^2 m^{-6}), a broadening that increases with increasing ℵ. That is, as ℵ becomes larger, not only are there ever increasingly larger values of *W*, but there is an increasing frequency of lower values of *W* as well. (As an aside, it is worth noting that the increased frequencies of larger *W* mean that there are locations enriched in cloud water for the enhanced growth of droplets lucky enough to encounter them.)

As one would anticipate, however, this is not dependent on χ_l (Fig. 6b) because the correlation has to do with the spatial relation among the realizations of concentrations rather than with the statistics of the droplet and water concentrations themselves. Nevertheless, the correlation length, χ_l, apparently plays some role in determining the distance over which $W > w_c$. This is illustrated in Fig. 7 for ℵ = 1 along the 10-km path. One of the reasons correlation lengths then become important is that longer χ_l means that $W > w_c$ over longer intervals so that there is a longer total path over which dense icing can occur. However, as w_c increases, the total length over which $W > w_c$ decreases for a fixed ℵ, as one might anticipate looking at Fig. 4. On the other hand, for a constant Schumann–Ludlam threshold, the total length over which dense icing is possible increases as the clustering intensity, ℵ, increases (Fig. 8) because of increasing frequencies of $W > w_c$.

There is a second significant effect of increasing ℵ, namely, that as ℵ becomes larger, any spongy ice that does form is then more likely to freeze rather than to slough off because of the greater frequency of relative voids deficient in cloud water. These regions will tend to promote heat loss with minimal compensating heat gains derived from the acquisition of significant amounts of new cloud water. Consequently, the freezing of previously accumulated water will be enhanced. This

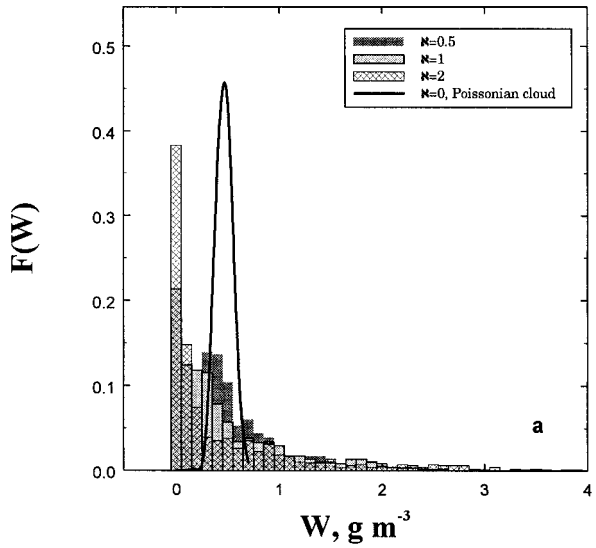

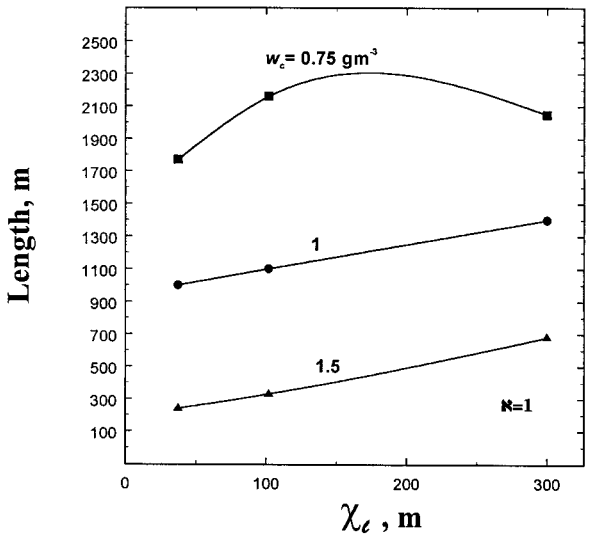

FIG. 7. The total length along a 10-km path of simulated clustered cloud over which W exceeds the indicated thresholds for a mean water content of 0.5 g m^{-3} as a function of the autocovariance length of the cloud water content for a fixed droplet clustering of $\aleph = 1$.

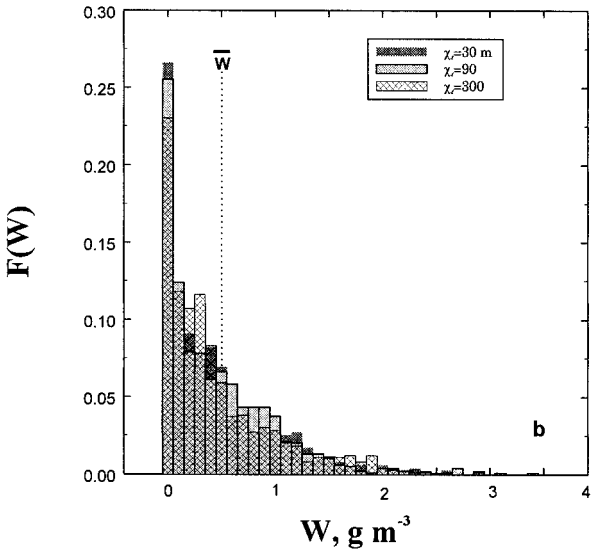

FIG. 6. (a) The frequency distribution for cloud water content for a mean of 0.5 g m^{-3} as a function of drop count clustering, $\aleph$, for a fixed χ_l of 300 m; and (b) the same except that $\aleph = 1$ and χ_l varies as indicated. Note that $F(W)$ is not affected by χ_l, as expected, but it does depend on $\aleph$. Also note the narrow distribution associated with a Poissonian cloud.

contrasts with a Poissonian cloud in which the heat gains and losses remain nearly steady.

Moreover, the accumulation of dense ice is further augmented in clustered clouds because as $\aleph$ increases, so do the cloud water contents associated with the clustering (Fig. 4). If one computes the total cloud water intercepted across a 1-cm^2 surface along 10-km paths in these simulations assuming that all the mass is completely collected where $w_c \geq 1$ g m^{-3} (a collection efficiency, E, of unity), then it is obvious (Fig. 9) that the amount of accumulated dense ice depends upon $\aleph$. In contrast, *no* dense ice accumulates if the droplet counts per unit volume are Poisson distributed (the Poissonian cloud) since the associated narrow distribution of W then means that the cloud water contents are always less than w_c.

Note, however, in Fig. 9, that χ_l appears much less

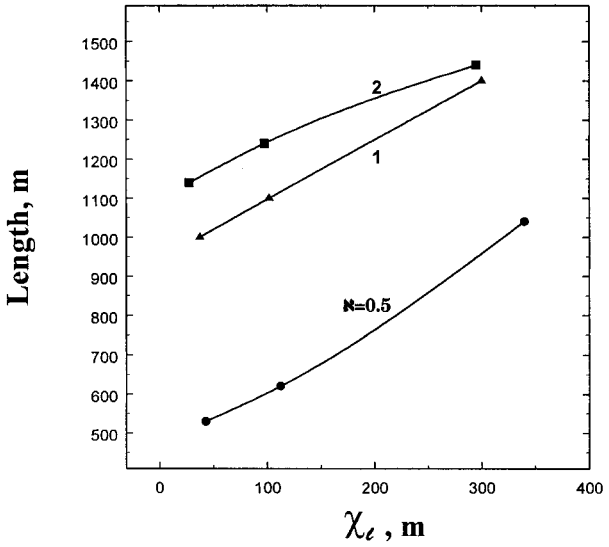

FIG. 8. Similar to Fig. 7 except that the threshold is fixed at 1 g m^{-3} while the clustering intensity is allowed to vary.

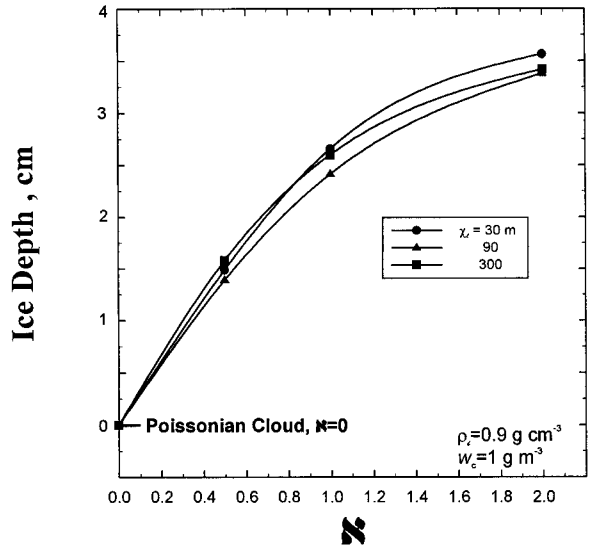

FIG. 9. The total depth of ice accumulated as a function of cloud droplet clustering along a 10-km path through a simulated cloud having a mean water content of 0.5 g m^{-3} assuming (i) all water is captured (a collection efficiency $E = 1$) and (ii) a Schumann–Ludlam threshold, w_c, of 1 g m^{-3}. Note that W for a Poissonian cloud never exceeds w_c.

important than $\aleph$ [at least when the sampling or ''measurement'' volume (in this case 10 m) is much less than χ_l] apparently because then $\aleph$, not χ_l, determines the availability of $W > w_c$. Since increased clustering is more likely where there is convection and turbulence, it is reasonable to conjecture that forecasts of where significant icing is likely must depend not only upon predictions of the locations of significant supercooled water contents but also upon the locations where convection and turbulence are likely to produce significant clustering.

4. Conclusions

In this work we explore the effect of cloud droplet clustering on the icing process. It is shown that it is not just the mean liquid water content but the variance to the mean ratio of W that is most important. Moreover, (6) and (7) imply that observed values of this ratio depend critically upon the length scale associated with the sampling volume.

Expressed somewhat differently, the fraction of the time that the cloud water content exceeds the critical value of the Schumann–Ludlam limit, w_c, will increase with increasing clustering intensity, $\aleph$. That is, the clustering of droplets leads to the clustering of cloud water content. What this means is that rather than being distributed as uniformly as randomness allows, the water is ''bunched'' into clumps of higher water concentration separated by relative voids deficient in cloud water where any accumulated spongy ice may then more readily freeze.

While rather academic at first glance, the introduction of such spatial inhomogeneities has some interesting effects. First, a point not really discussed in this work is that these inhomogeneities introduce a sense of direction to the icing process, where none exists in a Poissonian cloud. Specifically, if we consider a hailstone passing through a Poissonian cloud at a uniform temperature, the growth results are the same whether the hailstone moves from the beginning to the end point or vice versa. This is not the case for a clustered cloud because the growth rate is then no longer spatially uniform so that the path and direction become important. That is, a ''memory'' is introduced into the icing process by the clustering of the cloud droplets. As this work suggests (e.g., Fig. 9) such differences at times may have a profound effect on the growth of hail. Yet, clustering is a detail lost in the coarser resolution of most, if not all, numerical models.

More important, the analysis presented in this work is most relevant to situations when the temperature is nearly constant, as might happen as an aircraft flies at a constant altitude through a supercooled cloud. In that case, this work shows that quite significant icing can occur in a ''clustered'' as opposed to a ''Poissonian'' cloud having the same mean water content. The reason is that in a Poissonian cloud, the frequency distribution of the cloud water content is so narrow that fluctuations above the Schumann–Ludlam limit may never occur, as Fig. 9 illustrates. Yet in a clustered cloud, not only may such fluctuations become relatively frequent even for very modest levels of clustering, but both the size and the water contents of a cloud ''patch'' increase with increasing $\aleph$ and χ_l thereby significantly enhancing the potential accumulation of dense ice capable of altering the aerodynamics of an aircraft wing. Moreover, clustering promotes a freezing of any accumulated spongy ice in the relative voids between successive high water content patches.

Admittedly, Fig. 9 likely exaggerates the icing effects due to clustering since the collection efficiency is set to unity. Yet even a value of E as small as 0.1 in this example would still yield a significant ice thickness of about 0.2–0.4 cm. However, what is important here is not the detail of this particular simulation but rather the likelihood that such circumstances occur in nature. Specifically, from this study it is reasonable to conclude (i) that droplet clustering leads to significant broadening of the probability distribution of liquid water content; (ii) that significant dense ice formation may occur even when the mean supercooled liquid water content would suggest only low-density, dry rime for a Poissonian cloud; and (iii) that forecasting of conditions suitable for the formation of dense ice will depend not only on the prognosis of large-scale average supercooled cloud water contents but also on forecasting the variance of W at small scales presumably associated with significant convection and turbulence likely to enhance cloud clustering.

Acknowledgments. This work was supported by the National Science Foundation under Grants ATM95-12685 (AK), ATM94-19523 (AJ), and ATM97-12075 (AJ).

APPENDIX

A Procedure for Simulating Correlated Deviates for a Statistically Stationary, Homogeneous Process

While there are several techniques in the literature for generating correlated samples, the one used in this study is based upon that given by Johnson (1994). Although details may be found in that work, the approach is described here very briefly along the lines in Schulz and Kostinski (1997) and Koivunen and Kostinski (1999). Beginning with an exponential correlation function having coherence distance χ_l, the covariance matrix $\mathcal{K}_\rho$ is constructed as follows:

$$\mathcal{K}_\rho = \begin{bmatrix} \rho(0) & \rho(1) & \cdots & \rho(N) \\ \rho(-1) & \rho(0) & \cdots & \rho(N-1) \\ \vdots & \vdots & \ddots & \vdots \\ \rho(-N) & \rho(1-N) & \cdots & \rho(0) \end{bmatrix}, \quad \text{(A1)}$$

where $\mathcal{K}_\rho$ is symmetric, real, and Toeplitz (elements along each of the diagonals have the same value). If we then let $\mathcal{U}_\rho$ be the corresponding matrix of eigenvectors and Λ_ρ be the diagonal matrix of eigenvalues, or

$$\Lambda_\rho = \begin{bmatrix} \lambda_1 & 0 & \cdots & 0 \\ 0 & \lambda_2 & \cdots & 0 \\ \vdots & \vdots & \ddots & \vdots \\ 0 & 0 & \cdots & \lambda_N \end{bmatrix}, \quad \text{(A2)}$$

then the root matrix $\mathcal{H}_\rho$ of $\mathcal{K}_\rho$ is given by

$$\mathcal{H}_\rho = \mathcal{U}_\rho^{-1} \Lambda_\rho^{1/2} \mathcal{U}_\rho, \quad \text{(A3)}$$

where $\Lambda_\rho^{1/2}$ is a diagonal matrix with the elements $\lambda_\rho^{1/2}$ on the diagonal. Finally, if U_m is a sequence of mean zero, unit variance N random draws from, say the geometric distribution, then the transformed data υ_n given by

$$\upsilon_n = \sum_{m=1}^{N} \mathcal{H}_{\rho mn} u_m \quad \text{(A4)}$$

has the desired correlation properties (Johnson 1994). However, it is still necessary to adjust the variance to yield the desired $\aleph$ and to add the mean value to produce the final correlated series of statistically homogeneous drop concentrations. This is not as trivial as it seems, however, and involves some trial and error as well as several iterations at times. One begins first by multiplying to increase the variance appropriately. The mean is then added, and any negative counts are folded back into the data using the absolute value function. The mean is then readjusted, the data refolded, and so on until all values are positive, the mean is correct and we have the desired variance. Except in extreme cases, calculations show that this process conserves the proper correlation structure, $\aleph$, and χ_l, as demonstrated in Jameson and Kostinski (1999a,b).

However, since calculations using the cloud data described in Jameson et al. (1998) also indicate that not only are the droplets of one size correlated but so are droplets having different sizes, interdroplet correlation is assumed in this work. In order to preserve the cross correlation among different droplet sizes, the same procedure as above is used for each size category, except that the mean and variance are adjusted to account for changes due to the overall droplet size distribution (i.e., different mean concentrations for different sizes of droplets). Using the same sequence U_m assures a high degree of interdroplet cross correlation. This, of course, can also be adjusted to accommodate any degree of interdroplet decorrelation simply by modifying U_m. If, for some reason, no interdroplet cross correlation is desired, then one just uses independent, uncorrelated realizations of U_m.

In these simulations, the distribution of droplet counts is assumed to obey the geometric distribution (when $\aleph = 1$), the negative binomial distribution with $m = 2$ (when $\aleph = 0.5$) and stretch-exponential like distributions (when $\aleph = 2$), consistent with the cloud observations in Jameson et al. (1998) as well as rain drop observations in Kostinski and Jameson (1997), Jameson and Kostinski (1998), and Jameson et al. (1999). Regardless of the exact form, however, ''clustered'' clouds are always characterized by distributions having tails extending to larger counts usually much greater than for a Poisson distribution.

REFERENCES

Baker, B. A., 1992: Turbulent entrainment and mixing in clouds: A new observational approach. *J. Atmos. Sci.,* **49,** 387–404.

Green, H. S., 1969: *The Molecular Theory of Fluids.* Dover, 737 pp.

Jameson, A. R., and A. B. Kostinski, 1998: Fluctuation properties of precipitation. Part II: Reconsideration of the meaning and measurement of raindrop size distributions. *J. Atmos. Sci.,* **55,** 283–294.

——, and ——, 1999a: Non-Rayleigh signal statistics in clustered statistically homogeneous rain. *J. Atmos. Oceanic Technol.,* **16,** 575–583.

——, and ——, 1999b: Fluctuation properties of precipitation. Part V: Distribution of rain rates—Theory and observations in clustered rain. *J. Atmos. Sci.,* **56,** 3920–3932.

——, and ——, 2000: Fluctuation properties of precipitation. Part VI: Observations of hyperfine clustering and drop size distribution structures in three-dimensional rain. *J. Atmos. Sci.,* **57,** 373–388.

——, ——, and R. A. Black, 1998: The texture of clouds. *J. Geophys. Res.,* **103,** 6211–6220.

——, ——, and A. Kruger, 1999: Fluctuation properties of precipitation. Part IV: Finescale clustering of drops in variable rain. *J. Atmos. Sci.,* **56,** 82–91.

Johnson, G. E., 1994: Constructions of particular random processes. *Proc. IEEE,* **82,** 270–285.

Koivunen, A. C., and A. B. Kostinski, 1999: The feasibility of data whitening to improve performance of weather radar. *J. Appl. Meteor.,* **38,** 741–749.

Kostinski, A. B., and A. R. Jameson, 1997: Fluctuation properties of precipitation. Part I: On deviations of single-size drop counts from the Poisson distribution. *J. Atmos. Sci.,* **54,** 2174–2186.

——, and ——, 1999: Fluctuation properties of precipitation. Part III: On the ubiquity and emergence of the exponential drop size spectra. *J. Atmos. Sci.,* **56,** 111–121.

——, and ——, 2000: On the spatial distribution of cloud particles. *J. Atmos. Sci.,* **57,** 901–915.

Landau, L. D., and E. M. Lifshitz, 1980: *Statistical Physics.* Pergamon Press, 687 pp.

List, R., 1959: Wachstum von Eis-Wassergemischen im Hagel-versuchskanal. *Helv. Phys. Acta,* **32,** 293–296.

——, 1960: Zur Thermodynamik teilweise Wässrigger Hagelkörner. *Z. Angew. Math. Phys.,* **11,** 273–306.

Ludlam, F. H., 1958: The hail problem. *Nubila,* **1,** 12–96.

Macklin, W. C., 1961: Accretion in mixed clouds. *Quart. J. Roy. Meteor. Soc.,* **87,** 413–424.

——, 1962: The density and structure of ice formed by accretion. *Quart. J. Roy. Meteor. Soc.,* **88,** 30–41.

Paluch, I. R., and D. Baumgardner, 1989: Entrainment and fine-scale mixing in a continental convective cloud. *J. Atmos. Sci.,* **46,** 261–278.

Pruppacher, H. R., and J. D. Klett, 1997: *Microphysics of Clouds and Precipitation.* Kluwer Academic, 954 pp.

Schulz, T., and A. B. Kostinski, 1997: Variance bounds on the estimation of intensity and polarimetric parameters in radar meteorology. *IEEE Trans. Geosci. Remote Sens.,* **35,** 248–255.

Schumann, T. E. W., 1938: The theory of hailstone formation. *Quart. J. Roy. Meteor. Soc.,* **64,** 3–21.

Shaw, R. A., W. C. Reade, L. R. Collins, and J. Verlinde, 1998: Preferential concentration of cloud droplets by turbulence: Effects on the early evolution of cumulus cloud droplet spectra. *J. Atmos. Sci.,* **55,** 1965–1976.

Wang, L.-P., and M. R. Maxey, 1993: Settling velocity and concentration distribution of heavy particles in homogeneous isotropic turbulence. *J. Fluid Mech.,* **256,** 27–68.